A NUMERICAL STUDY OF NATURAL CONVECTION HEAT TRANSFER INSIDE A HORIZONTAL SQUARE ENCLOSURE WITH A CONCENTRIC HEATED ROD AND A BUNDLE OF TRIANGULAR HEATED CYLINDERS

Rana L. Natoosh
Mechanical Engineering Department - College of Engineering - Basra University

ABSTRACT:

In this paper, a numerical investigation of steady laminar natural convection in a square enclosure, contain a concentric heated rod and a bundle of four triangular heated cylinders was carried out. Two cases of enclosure inclination angle were studied: case (I) at $\varphi=0^o$ and case (II) at $\varphi=45^o$. Air is filled the enclosure, and the inner heated cylinders are located at equal distance (E) from the enclosure center. A finite element software package (FLEXPDE) is used in the present study to solve the set of non-linear equations governing the process. Solutions are obtained for aspect ratio h/H=0.29, a values of distance E=0.27-0.44 and a range of Rayleigh number $10^3 \leq Ra \leq 10^5$. The effect of Ra, E and φ were examined. Results are presented by streamlines, isotherms and Nusselt number and they indicates that the Nusselt number is significantly increases with increasing Ra, E and φ. A comparison of the streamlines, isotherms and mean Nusselt number was made with that obtained by other authors, which it reveals a good agreement.

KEYWORDS: Natural convection; Square Enclosure; Triangular heated cylinders; Uniform Wall Temperature

دراسه عدديه لانتقال الحرارة بالحمل الحر داخل فجوة افقيه مربعه تحوي انبوب مركزي مسخن مع حزمه مسخنه من القضبان المثلثه

رنى لطيف نتوش
قسم الهندسه الميكانيكيه - كليه الهندسه - جامعة البصره

الخلاصه

تمت في هدا البحث دراسة عددية للحمل الحر الطباقي المستقر في تجويف مربع الشكل يحوي اسطوانة مركزية مسخنة مع حزمة مسخنة من اربع اسطوانات مثلثة الشكل. تمت الدراسة لحالتين اعتماداً على زاوية ميلان التجويف الخارجي، الحالة الاولى عند الزاوية $\varphi=0^o$ والثانية عند $\varphi=45^o$. التجويف مملوء بالهواء والاسطوانات الداخلية مثبتة على ابعاد متساوية (E) من مركز التجويف . استخدمت طريقة الفروقات المحددة بمساعدة الحقيبة البرمجية (FLEXPDE) لحل المعادلات اللاخطية المتحكمة .الدراسة انجزت لنسبة ثابتة من ارتفاع المثلث الى ارتفاع التجويف الخارجي h/H=0.29 ، قيم المسافة E=0.27-0.44 ومدى رقم رايلي $10^3 \leq Ra \leq 10^5$. النتائج تمثلت بدلالة خطوط الجريان و خطوط التحارر ورقم نسلت ،حيث

اظهرت بان رقم نسلت يتاثر كثيرا" مع كل من E ، Ra وكدلك الزاويه φ . قورنت النتائج المستحصلة مع باحثين اخرين واظهرت تقارب جيد .

NOMENCLATURE

D	Diameter of circler rod (m)
E	The distance between the center of enclosure and triangular base
g	Gravitational acceleration (m/s^2)
h	Height of triangle (m)
H	Height of square enclosure (m)
Nu_L	Local Nusselt number
Nu_m	Mean Nusselt number
p,P	Pressure, dimensional(N/m^2) and dimensionless
Pr	Prandtl number
Ra	Rayliegh number
rr	Ratio of L/2ri
S	Dimensionless local coordinate
T	Temperature (K)
u, U	Dimensional and dimensionless horizontal velocity component
v, V	Dimensional and dimensionless velocity component
X,Y	Non-dimensional coordinates

Greek symbols

α	Thermal diffusivity (m^2/s)
β	Thermal expansion coefficient (1/K)
ε	The distance between the center of enclosure and the center of inner circular cylinder
θ	Dimensionless temperature
μ	Dynamic viscosity ($N/m^2.s$)
ν	kinematics viscosity (m^2/s)
ρ	Fluid density (kg/m^3)
φ	The angle of inclination of the enclosure
ψ	Stream function

Subscripts

i	inner
L	Local
m	mean
o	outer

1. INTRODUCTION

The phenomenon of natural convection in enclosures has received considerable attention in recent years. This attention is mainly because this phenomenon often affects the thermal performance in many engineering and science applications such as boilers, nuclear reactor systems, energy storage and conservation, fire control and chemical, food and metallurgical industries. In engineering applications, the geometries that arise however are more complicated than a simple enclosure filled with a convective fluid.

A large number of literature is available which deal with the study of natural convection in enclosures with either vertical (**Khaled and Bhattacharyy, 2006**), inclined (**Venkateswara et al.,2006), (Yasin et al., 2008**) or horizontal (**Natarajan et al, 2008**), (**Tanmay et al., 2009**) imposed temperature difference. (**Tanmay et al., 2009**) reported the numerical results of natural convection in trapezoidal enclosures for uniformly heated bottom wall, linearly heated vertical wall and of insulated top wall. Parametric studies for the wide range of Rayleigh numbers Ra ($103\text{-}10^5$) and Prandtl numbers Pr (0.7 -1000) with various tilt angles of side walls φ have been performed. It was found that, higher heat transfer rates for φ=0 and the overall heat transfer rates at the bottom wall were larger for the linearly heated left wall and cooled right wall. (**Patrick and Jane, 2005**) using an iterative, semi-implicit finite-difference method to solve the governing unsteady, three-dimensional free convective flow equations in a rectangular enclosure. The enclosure considered had rectangular horizontal lower and upper surfaces and vertical side surfaces and there were two square isothermal heated sections on the lower surface, the rest of this surface being adiabatic. (**Kim et al.2008**) studied the examine how the position of the inner circular cylinder relative to the outer square cylinder affects the natural convection phenomena for different Rayleigh numbers (

10^3–10^6) when a hot inner circular cylinder was located at different positions along the vertical centerline of the outer square cylinder. (**Kumar and Dalal, 2006**) considered the problem of natural convection around a square, horizontal, heated cylinder placed inside an enclosure in the range of $10^3 \leq Ra \leq 10^6$. Effects of the enclosure geometry have been assessed using three different aspect ratios placing the square cylinder at different heights from the bottom. (**Shu et al., 2001**) numerically studied natural convection between an outer square enclosure and an inner circular cylinder according to the eccentricity and angular position of the inner circular cylinder at a Rayleigh number of $3*10^5$. It was found that the global circulation, flow separation and the top space between the square outer enclosure and the circular inner cylinder have significant effects on the plume inclination. Laminar convection heat transfer from a horizontal triangular cylinder to its concentric cylindrical enclosure has been numerically studied by (**Zi-Tao et al., 2010**), to investigate the Prandtl number effect on flow and heat transfer characteristics. They found that the flow and heat transfer characteristics for a low Prandtl number fluid (Pr = 0.03) were unique and they were almost independent of Prandtl number when Pr ≥0.7. A numerical investigation of steady-state laminar natural convective heat transfer around a horizontal cylinder to its concentric triangular enclosure was studied by (**Xu Xu et al., 2010**). The enclosure was filled with air and both the inner and outer cylinders were maintained at uniform temperatures. At the highest Rayleigh number studied, the effects of different inclination angles of the enclosure and various cross-section geometries of the inner cylinder were investigated. The computed results indicated that at constant aspect ratio, both the inclination angle and cross-section geometry have insignificant effects on the overall heat transfer rates though the flow patterns are significantly modified. E. (**Fuad, 2009**) presented a numerical analysis of laminar natural convection in an enclosure of isosceles triangular cross-section has been performed for cold base and hot inclined walls. Base angles varying from 15 to 75 have been used for different Rayleigh numbers ranging from 10^3 to 10^5. It was observed that the enclosures with a low aspect ratio have higher heat transfer rates from the bottom surface of the triangular enclosure. (**Tanmay Basak et al., 2008**) used a finite element analysis with bi-quadratic elements to investigate the effects of uniform and non-uniform heating of inclined walls on natural convection flows within a isosceles triangular enclosure. The numerical solution of the problem was presented for various Rayleigh numbers (Ra), ($10^3 \leq Ra \leq 10^6$) and Prandtl numbers (Pr), ($0.026 \leq Pr \leq 1000$.

A survey of literature reveals that multi-inner triangular cylinders that are inside air-filled square enclosure has not been investigated. This is the motivation of the present study where a bundle of four triangular heated cylinders with concentric heated rod inside a square enclosure is to be studied. The effect of Rayleigh number, inclination angle of the enclosure and the distance between the center of enclosure and triangular cylinders on the flow and thermal fields for constant aspect ratio are studied in detail

2. GOVERNING EQUATIONS

A schematic of the two systems considered in the present study are shown in **Fig.1**. A case (I) **(Fig.1a)** consists a square enclosure ($\varphi=0^o$) while case (II) **(Fig.1 b)** consists a tilted square enclosure with $\varphi=45^o$. For two cases a square enclosure contains the concentric rod and four triangular cylinders located at equal distances E from the center of enclosure. The temperature of inner cylinders is higher than that of the square walls and both are uniform. The origin of the Cartesian coordinates (x, y) is positioned at a square center. The aspect ratios h/H=0.29 and D/H=0.24, the range of Rayliegh number $103 \leq Ra \leq 10^5$, the locations of the inner cylinder $0.27 \leq E \leq 0.44$ and Pr=0.71 were considered in this study. The fluid is assumed to have constant physical properties but obeys the Bussinesq approximation according to which the compressibility effect every where is neglected except for Buoyancy force term. Viscous dissipation and heat generation are absent. Hence, the two-dimensional, incompressible, steady state dimensionless governing equations using conservation of mass, momentum and energy can be written as (**Xu Xu et al., 2010**):

$$\frac{\partial U}{\partial X}+\frac{\partial V}{\partial Y}=0 \tag{1}$$

$$U\frac{\partial U}{\partial X}+V\frac{\partial V}{\partial Y}=-\frac{\partial P}{\partial X}+\frac{\partial^2 U}{\partial X^2}+\frac{\partial^2 U}{\partial Y^2} \tag{2}$$

$$U\frac{\partial V}{\partial X}+V\frac{\partial V}{\partial Y}=-\frac{\partial P}{\partial Y}+\frac{\partial^2 V}{\partial X^2}+\frac{\partial^2 V}{\partial Y^2}+\left(\frac{Ra}{\mathrm{Pr}}\right)\theta \tag{3}$$

$$U\frac{\partial \theta}{\partial X}+V\frac{\partial \theta}{\partial Y}=\frac{1}{\mathrm{Pr}}\left(\frac{\partial^2 \theta}{\partial X^2}+\frac{\partial^2 \theta}{\partial Y^2}\right) \tag{4}$$

Non-dimensional parameters can be given as follows:

$$X=\frac{x}{H},\quad Y=\frac{y}{H},\quad U=\frac{uH}{\upsilon},\quad V=\frac{vH}{\upsilon},\quad \theta=\frac{T-T_o}{T_i-T_o},\quad P=\frac{(p+\rho gy)H^2}{\rho v^2}$$

Prandtl number $\mathrm{Pr}=\frac{\upsilon}{\alpha}$, and Rayleigh number $Ra=\frac{g\beta(T_i-T_o)H^3}{\upsilon\alpha}$

3. NUMERICAL SOLUTION

It is well known in the numerical solution field that the set of equations (Eqs. (1) to (3)) may be highly oscillatory or even sometimes undetermined because of inclusion of the pressure term in the momentum equations. In the present study, a finite element software package (Flexpde) (**Backstrom, 2005**) is relied on in solution of the nonlinear system of equations. In finite element method there is a derived approach with purpose of stabilizing pressure oscillations and allowing standard grids and elements. This approach enforces the continuity equation and the pressure to give the following, what called penalty approach (**Langtangen, 2002**)

$$\nabla^2 P=\lambda\left(\frac{\partial U}{\partial X}+\frac{\partial V}{\partial Y}\right) \tag{5}$$

Where λ is a parameter that should be chosen either from physical knowledge or by other means (**Langtangen, 2002**). A most convenient value for λ was attained in this study to be $1E8\mu/H^2$. Hence, the continuity equation (1) is excluded from solution system and replaced by equation (5). The numerical solutions are obtained in terms of velocity components (U,V) and the stream function (ψ)is evaluated using the relationship between the stream function (ψ) and velocity components (U,V) as (**Tanmay et al., 2007**):

$$\frac{\partial^2 \psi}{\partial X^2}+\frac{\partial^2 \psi}{\partial Y^2}=\frac{\partial U}{\partial Y}-\frac{\partial V}{\partial X} \tag{6}$$

It may be noted that the positive sign of ψ denotes anti-clockwise circulation and the clock wise circulation is represented by the negative sign of ψ.

The heat transfer coefficient in terms of the local Nusselt number Nu_L along the inner cylinders surface and the outer wall is defined by (**Tanmay et al., 2007**):

$$Nu_L = -\frac{\partial \theta}{\partial n} \tag{7}$$

where n is the normal direction on a plane. At steady- state it is obvious that the mean Nusselt numbers along both the inner and outer walls are exactly identical. Hence, the average Nusselt number can be evaluated along the outer wall as:

$$Nu_m = \frac{1}{S_o}\int_{So} Nu_L dS_o \tag{8}$$

The appropriate boundary conditions are as follows
- Isothermal surfaces i.e. θ=1 on the concentric rod and triangular cylinders walls and θ=0 on the square walls.
-No-slip velocity boundary condition, U=V=0 on all solid walls.
-pressure gradient normal to all surfaces is zero, $\frac{\partial P}{\partial n} = 0$ where n is a normal unit vector.

4. VALIDATION

4.1 Software Validation

To check the validation of software, the grid dependency and the distribution values of ($\partial U/\partial X + \partial V/\partial Y$) over the domain $Ra=10^3$ and E=0.36 with accuracy 10^{-4} are presented in **Fig.2, a** and **b**. It is clear that the continuity equation is exactly validated, where it as mentioned in section 3, do not contribute in solving the governing equations.

4.2 Validation of numerical results

For the purpose of code validation, the natural convection problem for a low temperature outer square enclosure and high temperature inner circular cylinder ($Ra=3*10^5$, Pr=0.71, ($rr = L/2r_i$) equal to 2.6 (where L: side length of the square outer cylinder, r_i: radius of the inner cylinder) and the distance from the center of enclosure to the center of the inner cylinder ε =0, 0.25 and 0.5) was tested. The streamlines and isothermal patterns at ε =0.25 for present result are compared with the (**She et al., 2001**), see **Fig.3**. The results of the present work shows a good agreement with those of Ref. (**She et al., 2001**). The calculated mean Nusselt number Nu_m along the outer wall between the present work and the work of Ref.(**She et al., 2001**) is compared for ε =0, 0.25 and 0.5 as shown in **Table (1)** . The Nu_m are in good agreement with the values of (She et al., 2001).

5. RESULTS AND DISCUSSION

In the present study the effect of the Rayleigh number and the locations of the inner triangular cylinders were systematically investigated for two different cases of the square enclosure. The basic features of flow and heat transfer are analyzed with the help of isotherm and the streamline patterns. Local and average Nusselt numbers on the isothermal surfaces are plotted to evaluate the local and overall heat transfer process.

5.1 Analysis of Flow and Thermal fields

For all Rayleigh numbers at each case considered in this study, the flow and thermal fields are symmetric shape about the vertical centerline through the center of the concentric circular rod. In other words, the governing equations given in Eqs (1) to (4) and the boundary conditions are invariant to the following transformation:

Symmetry about x =0 : { u,v,θ,x,y} ⟵ { -u,v,θ,-x,y} (9)

5.1.1 Flow and thermal fields when E=0.36

The results of flow fields and isotherms for air flow in a square with heated inner cylinders at E=0.36 are examined in this section.

Fig.4 shows streamlines (on the left) and isotherms (on the right) for different values of Ra in case(I) (φ=0). At low Ra ($Ra=10^3$), as shown in the left side in **Fig.4a**, six circulation cells of streamlines are formed inside the enclosure. Two of them are the strongest and localized in the space between each two triangular cylinders near the vertical walls. The others are smaller and located around a concentric rod. This formula of circulations are appear due to the buoyant effects which are caused by the temperature difference between the inner and outer walls, and this lead to form the recirculation vortices which are clearly demonstrated by the closed streamlines. At $Ra=3*10^4$, as shown in the left side of **Fig.4b**, it can be seen that the upper and lower cells around concentric rod merge together and a new cell is formed near each corner of the enclosure. As Ra increases to 10^5(**Fig.4c** on left), the cells in the upper two corners begin to merge with the two strong cells while two small new cells appears near the upper part of concentric rod when the old two cells begin to move down . The effect of buoyancy force become stronger compared to viscous forces and the intensity of fluid motion has been increased as indicated by relatively larger magnitudes of stream functions.

The thermal fields are presented in the form of isotherms in the right side of **Fig.4**. At $Ra=10^3$(**Fig.4a**), the heat transfer in the enclosure is mainly dominated by the conduction mode therefore, we can observe that four equivalent like plumes distribution start to appears from the space between each two inner triangular cylinders towards the center of enclosure. With increasing of Rayliegh number ($Ra=3*10^4$) as shown in **Fig.4b**, the upper plume vanish gradually while the lower plum start to growth toward the center of enclosure. As the Rayleigh number increases up to 10^5, the role of convection in heat transfer becomes more significant, consequently the upper plum disappear while the lower and both side plumes rise upward , giving rise to a stronger thermal gradient in the upper part of the enclosure.

Fig.5 shows streamlines (on the left) and isotherms (on the right) for different values of Ra in case (II) (φ=45). At low Ra ($Ra=10^3$) ,as in case(I), there are many circulation cells formed inside the enclosure and the number of cells here is larger than in case(I) , this is because of the inclination of the enclosure that leads to increase of the secondary flow. Two small circulation cells localized in the space between each triangular cylinder side and enclosure corners, another two cells appears at each side of the concentric rod. The last four circulation cells are more in strength and localized in the space between each two inner triangular cylinders. With increasing of Rayleigh number ($Ra=3*10^4$and $Ra=10^5$),as shown in **Fig.5b** and **c**, the size of the small cells are growth and the two cells near the concentric rod start to move upward, also the two cells that are in the upper part of the enclosure slightly becomes smaller in size and weaker in strength compared with those in lower part of it. As in case(I), the strength of cells become more at high Rayleigh numbers compared with the lower values of it, due to increase the buoyancy effect and dominant of free convection heat transfer.

The behavior of thermal patterns in this case is similar to that in case (I) especially at $Ra=10^3$, as shown the right side in **Fig.5**. At $Ra=3*10^4$ we can observe in **Fig.5b** that the size of each upper like plum distribution is vanish gradually with increasing of Rayleigh number. For high Rayleigh number ($Ra=10^5$)as shown in **Fig.5c**(right), the lower plumes start to growth to upward and merge with the upper plumes due to reducing the density of fluid which lead to growth the thermal boundary layer.

5.1.2 Flow and temperature fields as a function of E:-

The dependence of the flow and thermal fields on the location of inner heated triangular cylinders can be observed in the plots of the streamlines and isotherms for three different values of E (0.27, 0.36, 0.44) at $Ra = 3*10^4$ and φ=0 (case(I)) as shown in **Fig.6**. It can be seen from the left side of this figure that the number of circulation cells decreases with increasing the value of E while the size of each cells increases with increasing of E. This is because a greater space is then available

for the cells to be larger when E increases. It is also noticed that the strength of cells increases with increasing of E. The right side of **Fig.6** shows that the upper like plum distribution is vanish at lower values of E (E=0.27) while the size of each plum increases with increasing of E due to the increasing the growth of the thermal boundary layer

5.2 Heat transfer rates: local and mean Nusselt numbers

5.2.1 Local Nusselt numbers

Figs.7 and **8** display the effects of Ra on the local Nusselt number along the circumference of inner triangular cylinders and outer enclosure wall for E=0.36 in case (I) and case (II) respectively.

Variation of the local Nusselt number along the upper left inner triangular cylinder at φ=0 for different Rayleigh numbers is plotted in **Fig.7-A**. As can be seen from this figure that, at $Ra=10^3$ the local Nusselt number (Nu_L) has a maximum value at $S_1=0$, which represent the point on the upper left corner of the triangular, then the Nu_L decreases until $S_1=0.11$, and it remain constant to the distance $S_1=0.22$, then the Nu_L increases until $S_1=0.29$, which represent the point on the lower corner of the triangular cylinder. When we move along the inclined wall of the triangular cylinder, the value of Nu_L decreases, and reaches a minimum at $S_1=0.5$, then increases toward the upper right corner at $S_1=0.71$. Then the turned of curve of Nu_L along the horizontal surface of triangle ($0.71\leq S_1\leq 1$) is the same as that of vertical wall. The shape of the local Nusselt number distribution at $Ra=3*10^4$ is generally similar to that at $Ra=10^3$. At high Rayleigh number ($Ra=10^5$), the distribution is different along the inclined and horizontal walls of the triangular cylinder. The values of Nu_L increases with increasing of Ra along the portion $0.3\leq S_1\leq 0.62$ and decreases otherwise. This is due to the like plum distribution of the isotherms through the space between the heated cylinders (which is shown in **Fig.4**) is greatly spread at high Ra due to the increase the strength of streamlines. The maximum values of Nu_L appear on the corners of the triangular cylinder, due to the growth of thermal boundary layer near the corners and that's lead to dominant the convection instead of conduction near to these regions. **Fig7-B** shows the distribution of local Nusselt numbers along the lower left inner triangular cylinder for different Rayleigh numbers. The curves have a similar U-shape at each wall of the triangle. The value of Nu_L has a relatively small variation with increasing of Ra along the vertical and inclined walls of the triangular cylinder while it increases with increasing of Ra along the horizontal wall. The higher values of Nu_L appears at the vertical and horizontal walls due to the dominant of convection near to these regions, while the values of Nu_L are lower at the inclined wall of triangular cylinder due to the dominant of conduction. The distribution of Nu_L along the concentric rod for the same parameters above is shown in **Fig.7-C**. At $Ra = 10^3$, the distribution of Nu_L show almost a symmetric shape with respect to the horizontal centerline at y = 0 due to the symmetric distribution of isotherms. The variation of Nu_L is very small and increases with increasing Ra. With increasing of Rayleigh number ($Ra=3*10^4$ and 10^5) the distribution of Nu_L is not symmetric any more with respect to horizontal due to the effect of convection. Also we can observe that the maximum value of Nu_L appears at $S_i=0.5$ while the minimum values at the upper point of cylinder ($S_i=0$ or $S_i=1$) .The maximum value of local Nusselt number increases with increasing Ra because the like plumes distribution growth upward in the presence of convection, meaning that the Nu_L at the lower surface of the concentric rod is larger than that at the upper surface of it. Variations of the local Nusselt number along the outer enclosure wall are plotted in **Fig.7-D** for the same above parameters. The curves have a similar sinusoidal distribution with M-shape at the distance which represents the base and each vertical side of the square enclosure. The distribution of Nu_L at the upper surface of enclosure changes with increasing of Ra. At $Ra=10^3$ the Nu_L on the upper wall have the same behavior while when Ra increases to 10^5, the behavior of Nu_L is completely different having sinusoidal distribution with very high values of Nu_L. This different due to the growth the plumes to upward as shown in **Fig.4**(on left), and as a result the values of local Nusselt number along the upper part of enclosure wall ($0 \leq S_o\leq 0.125$ and $0.625 \leq S_o\leq 1$) is larger than that at the lower part of it ($S_o=0.125$-0.625).

Fig. 8-A shows the distribution of local Nusselt numbers along the hot surface of the upper triangular cylinder for different Ra and $\varphi=45^{o}$. The distribution of Nu_L shows symmetrical shape with respect to the vertical centerline due to the symmetric shape distribution of flow and thermal fields. The distribution of Nu_L in this case is similar to that along the upper left triangular cylinder in case (I) , especially at lower values of Ra. Also it can be seen that the values of Nu_L decreases with increasing of Ra except along the portion that represents the bottom wall of the triangular cylinder ($0.29\leq S_1 \leq 0.71$). The maximum values of local Nusselt numbers appears at the upper corner of the triangle ($S_1=0$ or $S_1=1$) while the minimum values appears at $S_1=0.5$ due to the growth of the thermal boundary layer and dominant convection heat transfer near the upper corner while the conduction heat transfer is the dominant near the bottom wall of the triangular cylinder (as showed in **Fig.5**). The variation of local Nusselt numbers along the hot surface of the left triangular cylinder for different Ra are shown in **Fig.8-B**. It can be seen that the Nu_L is increases with increasing Ra along the lower inclined and the vertical walls of the triangular cylinder ($0.29\leq S_2 \leq 0.96$), while vise versa for the upper inclined wall. The lower values of Nu_L appears at the vertical wall due to dominant the conduction near the center of enclosure, while the values of Nu_L are higher at the lower inclined wall of triangular cylinder due to dominant of the convection. The distribution of local Nusselt numbers along the hot surface of the lower triangular cylinder for different Ra are shown in **Fig.8-C**. The distribution of Nu_L is similar to that along the lower left cylinder in case(I). The value of Nu_L increases with increasing of Ra along the left and right inclined walls of the triangular cylinder due to increasing the effect of convection, while it has a relatively small variation with increasing of Ra along the horizontal wall. The maximum value of Nu_L is located on the corner of triangular cylinder that is near the enclosure corner at $Ra=10^3$ and $Ra=3*10^4$. At $Ra=10^5$, the maximum values of Nu_L are located on each upper corner of triangular cylinder, because the isotherms are symmetric shape with respect to the vertical centerline at $x = 0$ as shown in **Fig.5**(left). Variation of the local Nusselt number along the concentric rod for the same above parameters is plotted in **Fig.8-D**. At $Ra=10^3$,as in case(I), the distribution of Nu_L show almost a symmetric shape with respect to the horizontal centerline at y=0 because the dominant effect is conduction. The other curves show two peaks with equal altitude at the left and right sides of the lower part of cylinder. The local Nusselt number increases with increasing Ra except along the upper part of the cylinder because, as previous mentioned, the lower plumes start to growth to upward in the presence of convection as shown in the left side of **Fig.5** .The maximum values of Nu_L, for $Ra=3*10^4$ and $Ra=10^5$, appears at $S_i=0.37$ and $S_i=0.63$ while the minimum values of Rayleigh number $10^3\leq Ra\leq 10^5$, appears at the upper point of concentric rod ($S_i=0$ or $S_i=1$). **Fig.8-E** shows the distribution of local Nusselt number along the outer enclosure wall for the same above parameters. For $Ra=10^3$ and $3*10^4$, the distribution exhibits the same form to that along the outer enclosure wall in case (I). At high Rayleigh number ($Ra=10^5$), the distribution of Nu_L along each the lower inclined walls of the square enclosure have the same behavior, while the behavior of Nu_L along each the upper inclined walls have sinusoidal distribution with very high values of Nu_L. This can be demonstrated by the steep temperature gradient along the upper inclined walls of enclosure as in **Fig.5c** right.

5.2.2 Mean Nusselt numbers

The mean Nusselt number is utilized to represent the overall heat transfer rate within the domain interest. **Fig.9a** and **b** shows the mean Nusselt number of the enclosure as a function of the distance (E) with different Rayleigh numbers for case (I) and case (II) respectively. It can be seen that the mean Nusslet number ,for each case, depends on the variation of the distance (E) and increases with increasing E, due to increasing the thermal gradient with decreasing the space between the inner cylinders and the wall of the outer enclosure as shown in **Fig.6** (right). Also we can observe from this figure that for each value of E the value of mean Nusselt numbers is increased with Ra due to dominant the convection heat transfer, and this value of increasing is greater in case(II) than in case(I) for $Ra\geq 10^4$ as illustrated more in **Fig.10**. The change of mean Nusselt numbers, at the outer enclosure, versus Ra with different (E) for each case is presents in Fig.10. It can be seen that,

for E=0.27 and E=0.36 the Nu_m is a strongly effected by high various of Rayliegh number especially in case(II) due to the growth of thermal boundary layer and enhancing the heat transfer coefficient. Also for E=0.44 we can observe that a small variation of Nu_m with increasing of Rayleigh number.

6. CONCLUSIONS

In the present paper, a numerical investigation of steady laminar natural convection in a square enclosure contain a concentric heated rod and a bundle of 4-trainguler heated cylinders was studied in two cases depending on various inclined angle of the enclosure ($\varphi=0^o$ and $\varphi=45^o$). A detailed analysis for the distribution of streamlines, isotherms and Nusselt number was carried out to investigate the effect of the locations of the heated inner cylinders on the fluid flow and heat transfer in the square enclosure for different Rayleigh numbers in the range of $10^3 \leq Ra \leq 10^5$. The conclusions can be drawn as follows:

1. Flow fields and isotherms are strongly affected by changing Rayleigh number, the location of inner cylinders (E), and the angle of inclination of the enclosure (φ).
2. The values of local Nusselt number along the upper part of outer enclosure wall are larger than that at the lower part of it.
3. The mean Nusselt number and the intensity of stream are an increasing function to Rayliegh number.
4. Location of the inner heated cylinders play an important role to enhance the over all heat transfer significantly.
5. The values of Nu_m in inclined square enclosure at $\varphi=45^o$ are larger than in enclosure at $\varphi=0^o$.

REFERENCES

-Backstrom Gunnar, (2005) "Fields of Physics by Finite Element Analysis Using FlexPDE" by GB Publishing and Gunnar Backstrom Malmo.

- Fuad Kent E.,(2009) "Numerical analysis of laminar natural convection in isosceles triangular enclosures for cold base and hot inclined walls" Mechanics Research Communications 36, 497–508.

-Khaled Khodary , Bhattacharyy, T.K., (2006) "Optimum natural convection from square cylinder in vertical channel" International Journal of Heat and Fluid Flow 27, 167–180

- Kim B.S. , Lee D.S., Ha M.Y. ,Yoon H.S., (2008) "A numerical study of natural convection in a square enclosure with a circular cylinder at different vertical locations" International Journal of Heat and Mass Transfer 51, 1888–1906.

- Kumar De A., Dalal A., (2006) "A numerical study of natural convection around a square, horizontal, heated cylinder placed in an enclosure "Int. J. Heat Mass Transfer 49, 4608–4623.

-Langtangen H.P., Mardal K.A. and Winther R., (2002) " Numerical methods for incompressible viscous flow" Advances in Water Resources 25 1125–1146.

- Natarajan E., Tanmay Basak, Roy S.,(2008) "Natural convection flows in a trapezoidal enclosure with uniform and non-uniform heating of bottom wall" International Journal of Heat and Mass Transfer 51, 747–756.

- Patrick H. Oosthuizen , Jane T. Paul, (2005) "Natural convection in a rectangular enclosure with two heated sections on the lower surface"International Journal of Heat and Fluid Flow 26, 587–596.

- Shu C., Xue H., Zhu Y.D.,(2001) "Numerical study of natural convection in an eccentric annulus between a square outer cylinder and a circular inner cylinder using DQ method" Int. J. Heat Mass Transfer, 44, 3321–3333.

-Tanmay Basak, Roy S., Amit Singh, Bishun D. Pandey, (2009) "Natural convection flow simulation for various angles in a trapezoidal enclosure with linearly heated side wall(s)" International Journal of Heat and Mass Transfer 52, 4413–4425.

- Tanmay Basak, Roy S., Krishna Babu S., Balakrishnan A.R., (2008) "Finite element analysis of natural convection flow in a isosceles triangular enclosure due to uniform and non-uniform heating at the side walls" International Journal of Heat and Mass Transfer 51, 4496–4505.

- Tanmay Basak, Roy S., Thirumaleshaa Ch., (2007) " Finite element analysis of natural convection in a triangular enclosure: Effects of various thermal boundary conditions" Chemical Engineering Science 62, 2623 – 2640

- Venkateswara Rao M., PV Ravi Kumar&PSI Sankara Rao , (2006) "laminar flow heat transfer in concentric equilateral triangular annular channel", Indian Journal of Chemical Technology Vol.13, pp.614-622.

- Xu Xu , Zitao Yu , Yacai Hub, Liwu Fan , Kefa Cen, (2010) "A numerical study of laminar natural convective heat transfer around a horizontal cylinder inside a concentric air-filled triangular enclosure" International Journal of Heat and Mass Transfer" International Journal of Heat and Mass Transfer 53, 345–355.

- Yasin Varol, Hakan F. Oztop and Ioan Pop, (2008) "Numerical analysis of natural convection in an inclined trapezoidal enclosure filled with a porous medium" International Journal of Thermal Sciences 47, 1316–1331.

-Zi-Tao Yu, Li-Wu Fan , Ya-Cai Hua, Ke-Fa Cen,(2010) "Prandtl number dependence of laminar natural convection heat transfer in a horizontal cylindrical enclosure with an inner coaxial triangular cylinder" International Journal of Heat and Mass Transfer 53, 1333–1340.

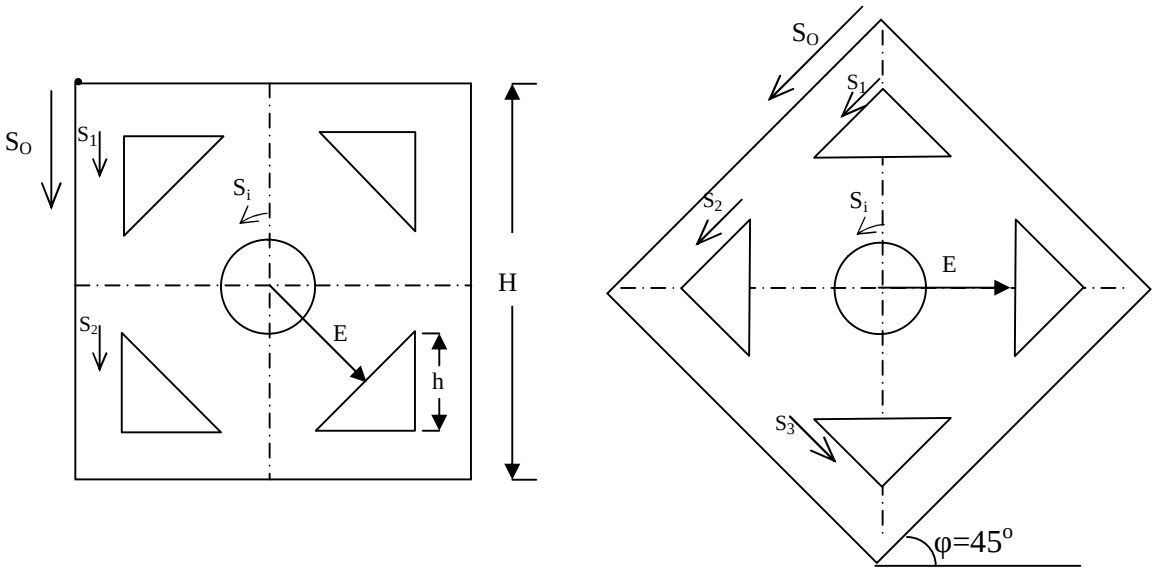

-a- -b-

Fig.1 schematic diagrams of the physical domain a) case(I) b) case(II)

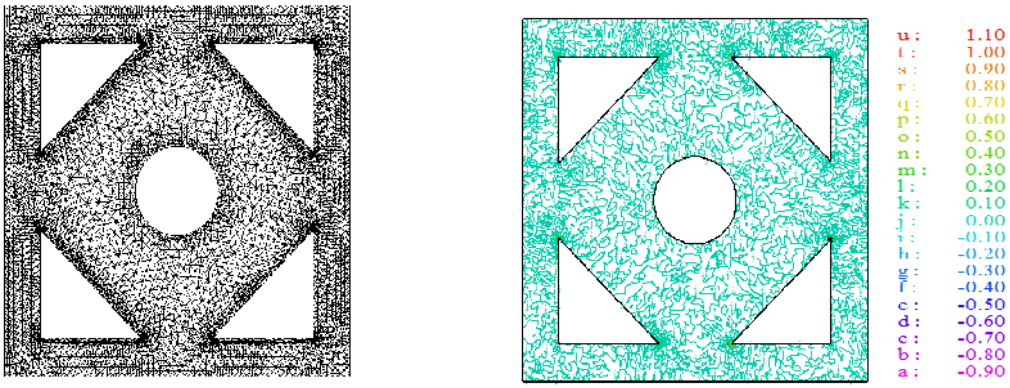

-a- -b-

Fig.2 (a) grid distribution over the domain (b) validation of continuity equation

Table (1) Comparison of Nu_m between the present work and the work of (Shu et al., 2001) for $Ra=3*10^5$, pr=0.71 and rr=2.6

ε	Nu_m (present)	Nu_m (Shu et al., 2001)	Error %
0	6.6	6.52	1.2
0.25	6.689	6.75	0.903
0.5	6.95	6.98	0.43

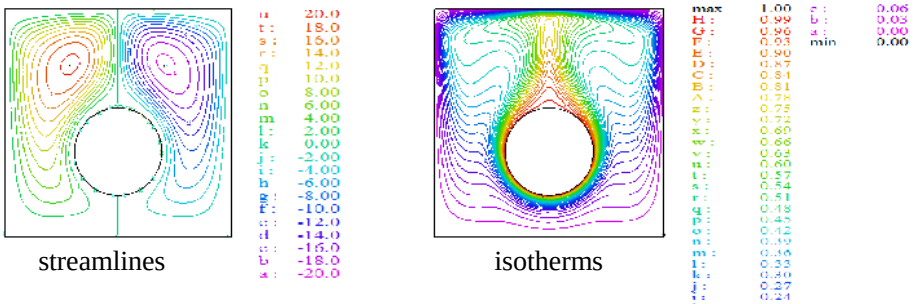

Present work

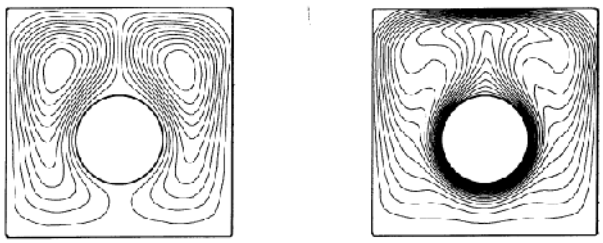

Shu et al.(2001)

Fig.3 comparison of streamlines and isotherms with (**Shu et al., 2001**) for $Ra=3*10^5$, Pr=.71, and rr=2.6

a

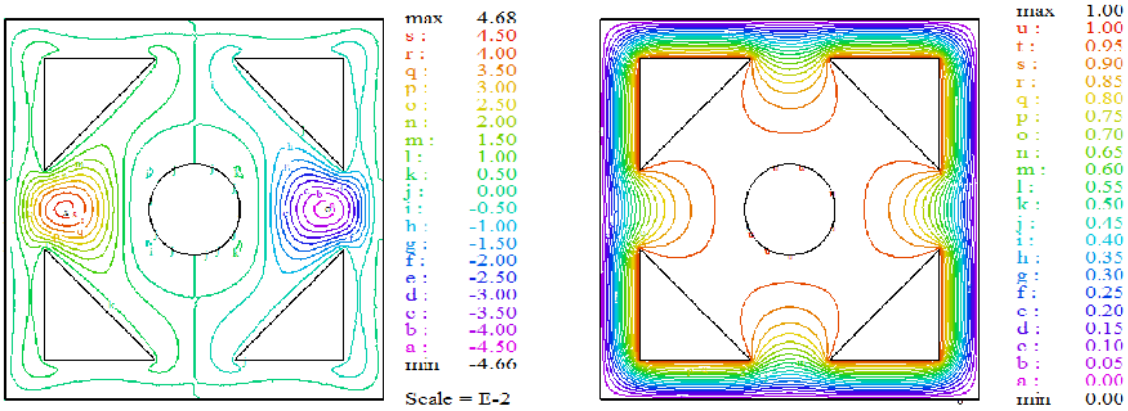

b

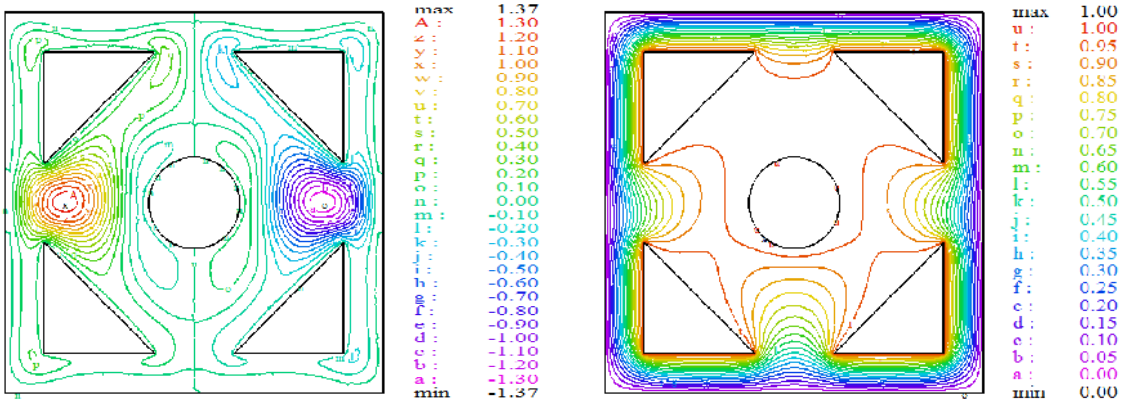

c

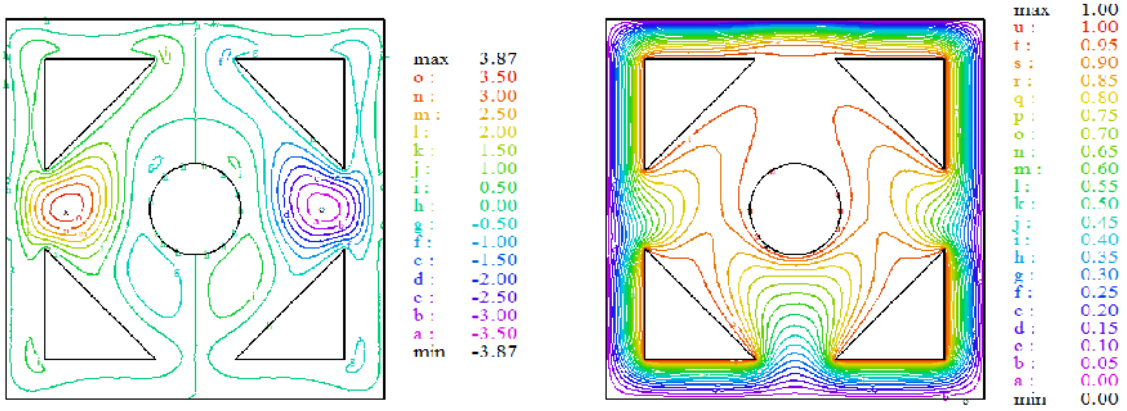

Fig.4 Streamlines (left) isotherms (right) for case(I) a)$Ra=10^3$ b)$Ra=3*10^4$ c) $Ra=10^5$

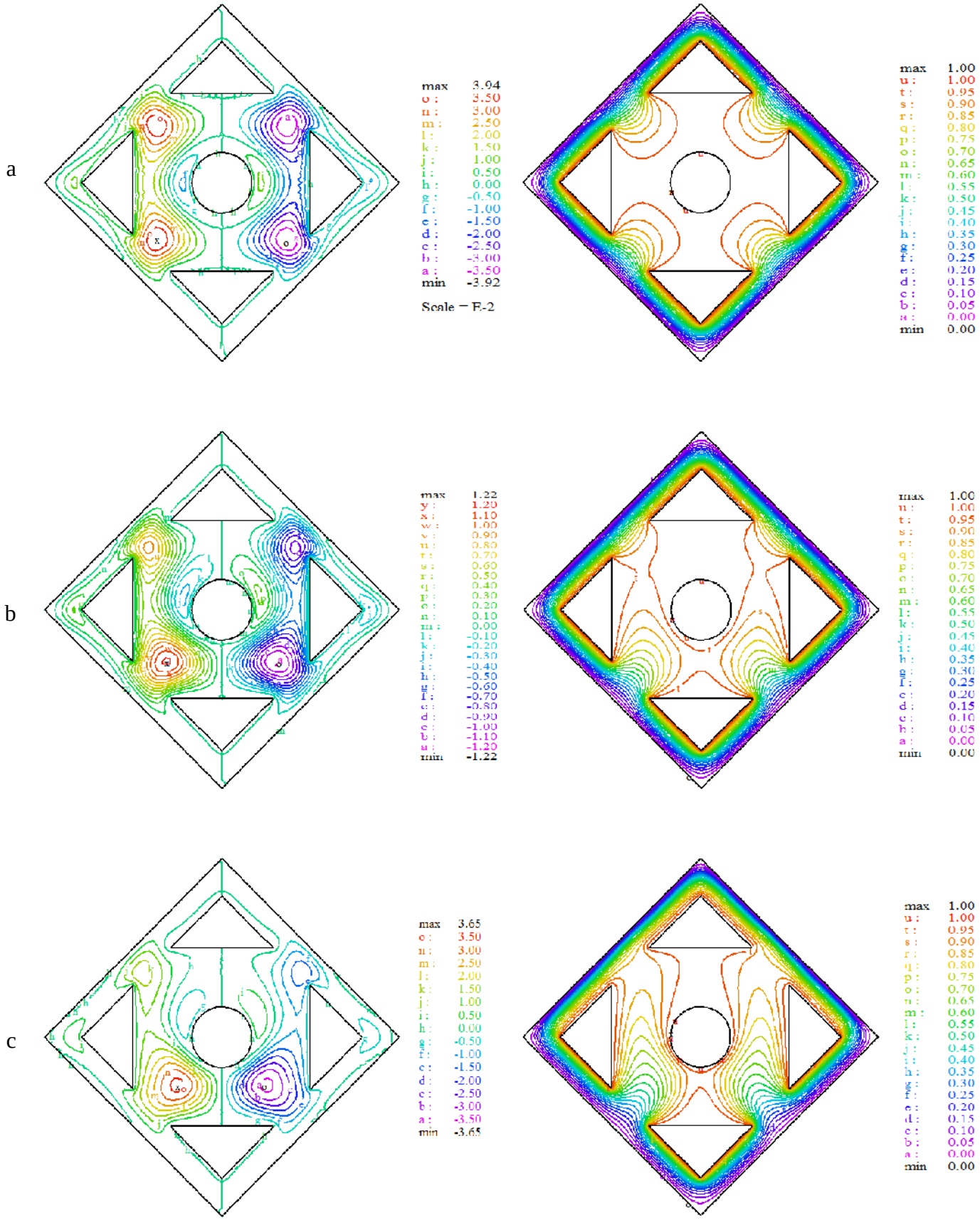

Fig.5 Streamlines (left) isotherms(right) for case(II) a)$Ra=10^3$ b)$Ra=3*10^4$ c) $Ra=10^5$

a

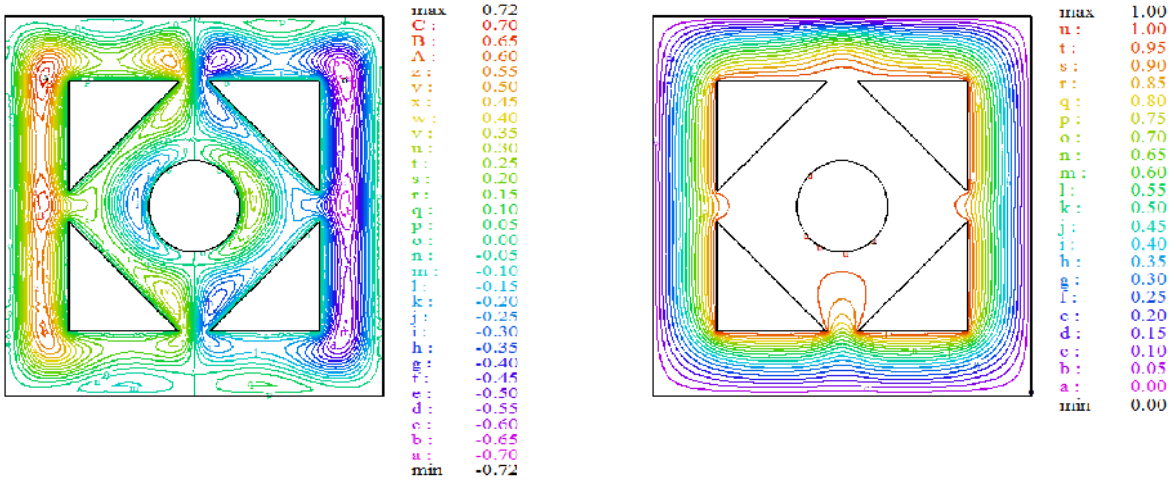

b

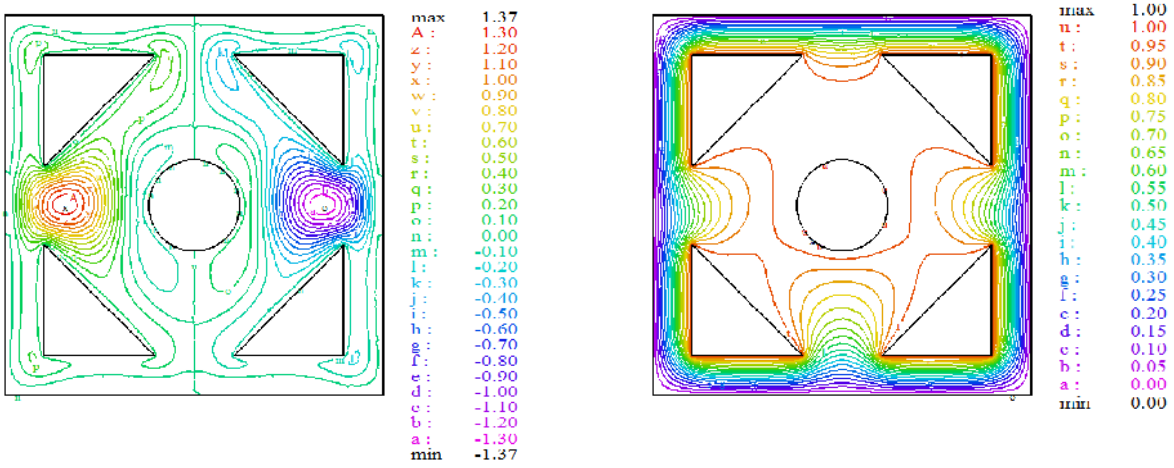

c

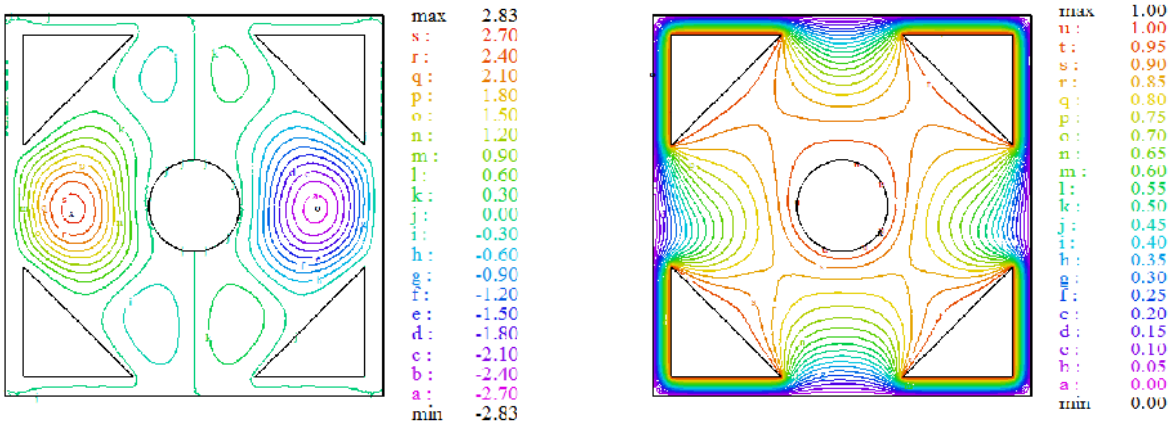

Fig.6 Streamlines(left) and isotherms (right) for case(I) and $Ra=3*10^4$
a)E=0.27 b)E=0.36 c)E=0.44

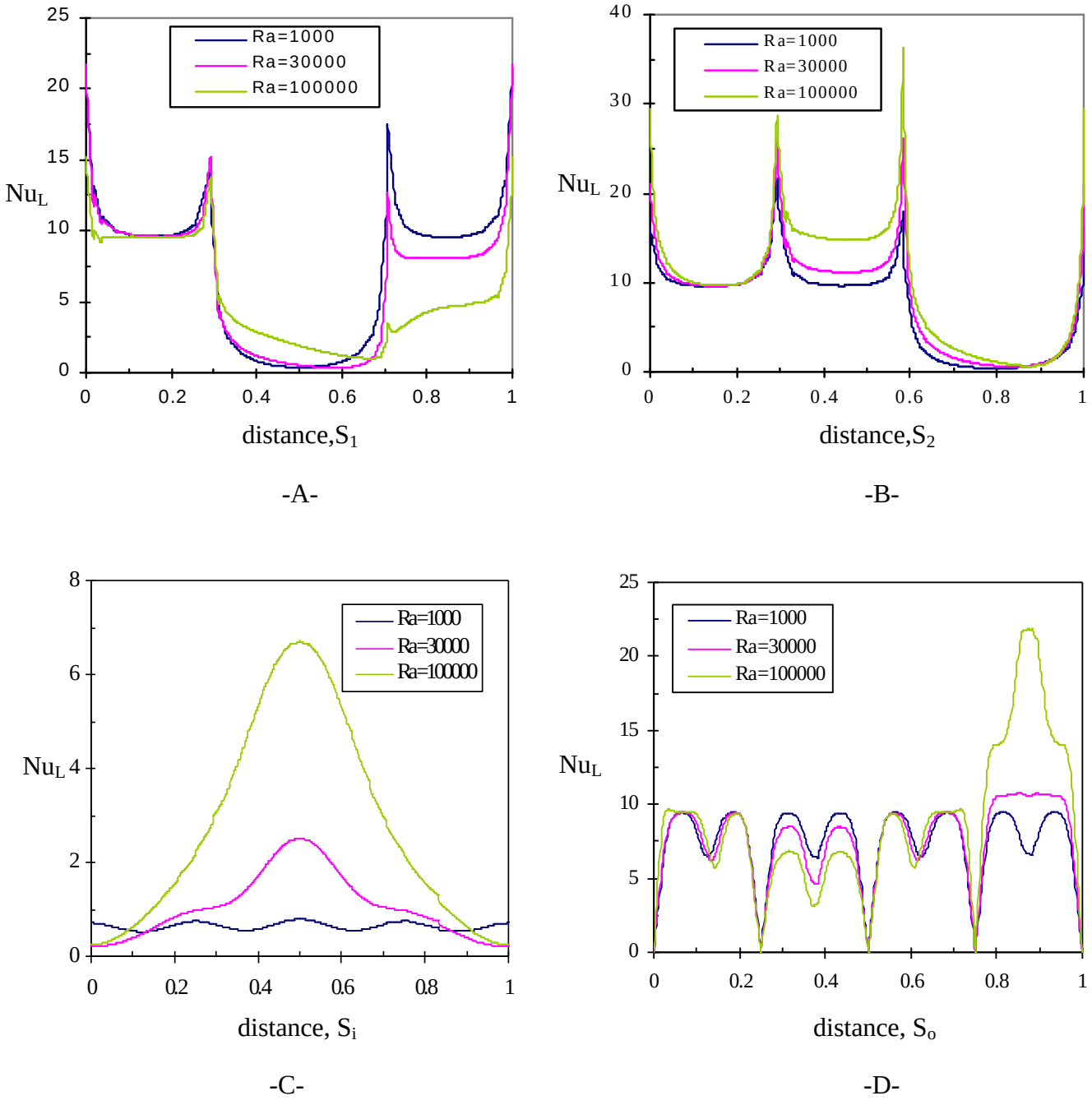

Fig.7 Variation of the local Nusselt number for case(I) along the
A) upper left triangular cylinder B) lower left triangular cylinder
C)concentric circular rod D)outer enclosure,
at E=0.36

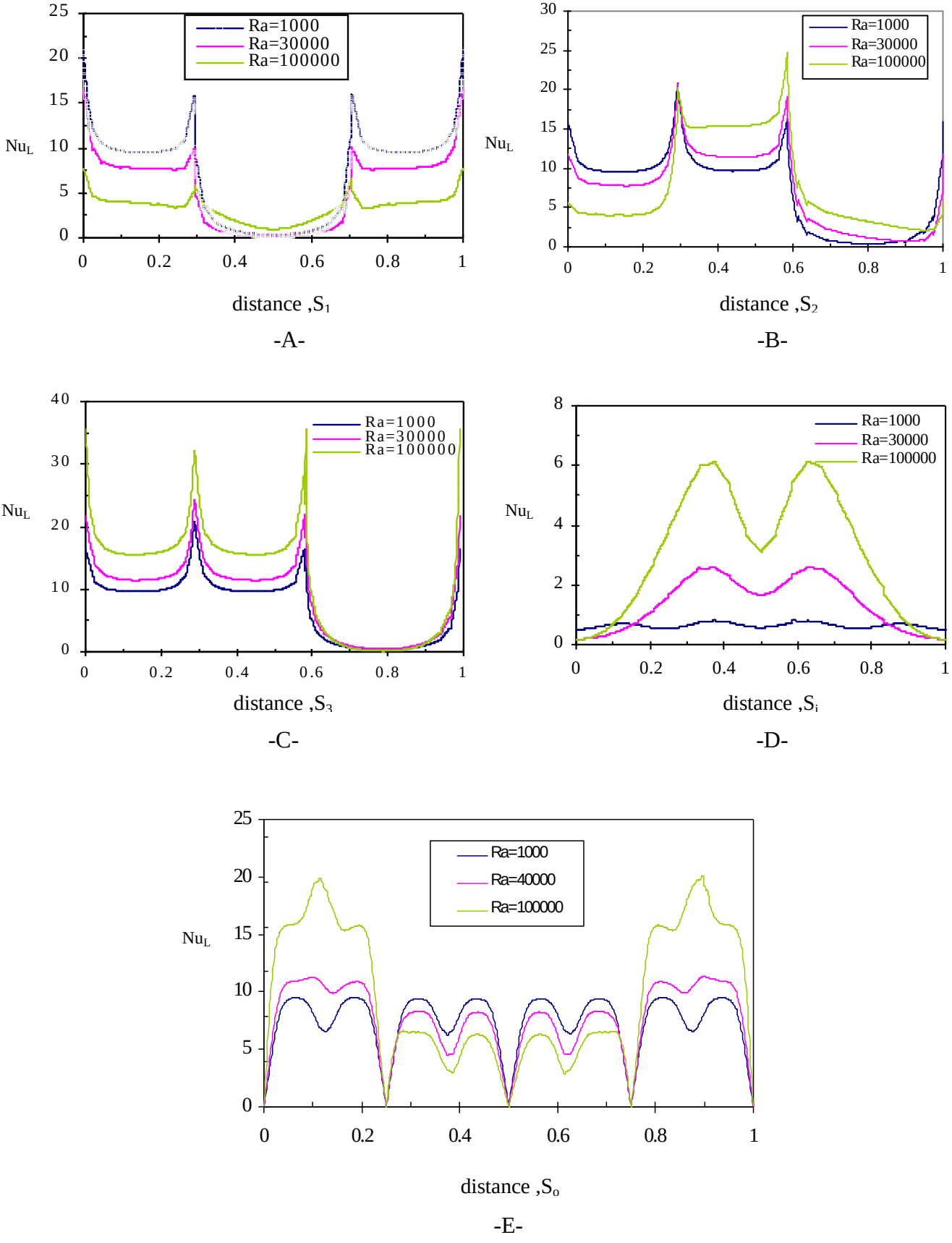

Fig.8 Variation of the local Nusselt number for case(II) along the A) upper triangular cylinder B) left triangular cylinder C)lower triangular cylinder D) concentric circular rod E) outer enclosure, at E=0.36

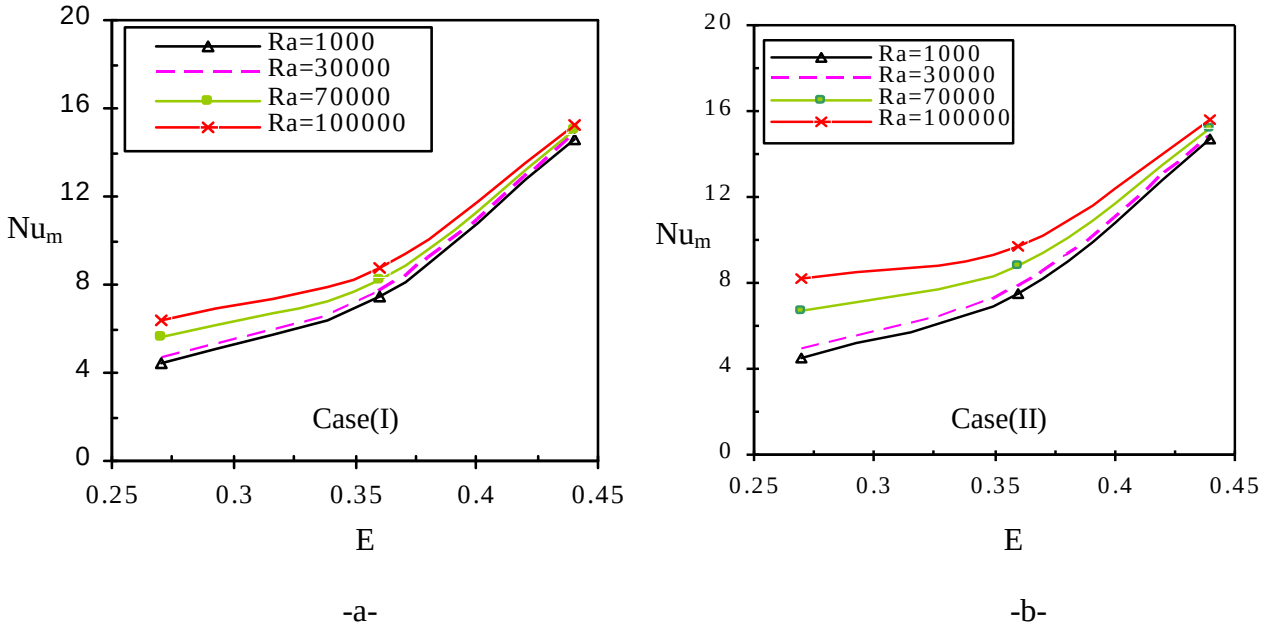

Fig.9 Variation of the mean Nusselt number with E along the outer wall for different Rayleigh number a) case(I) b) case(II)

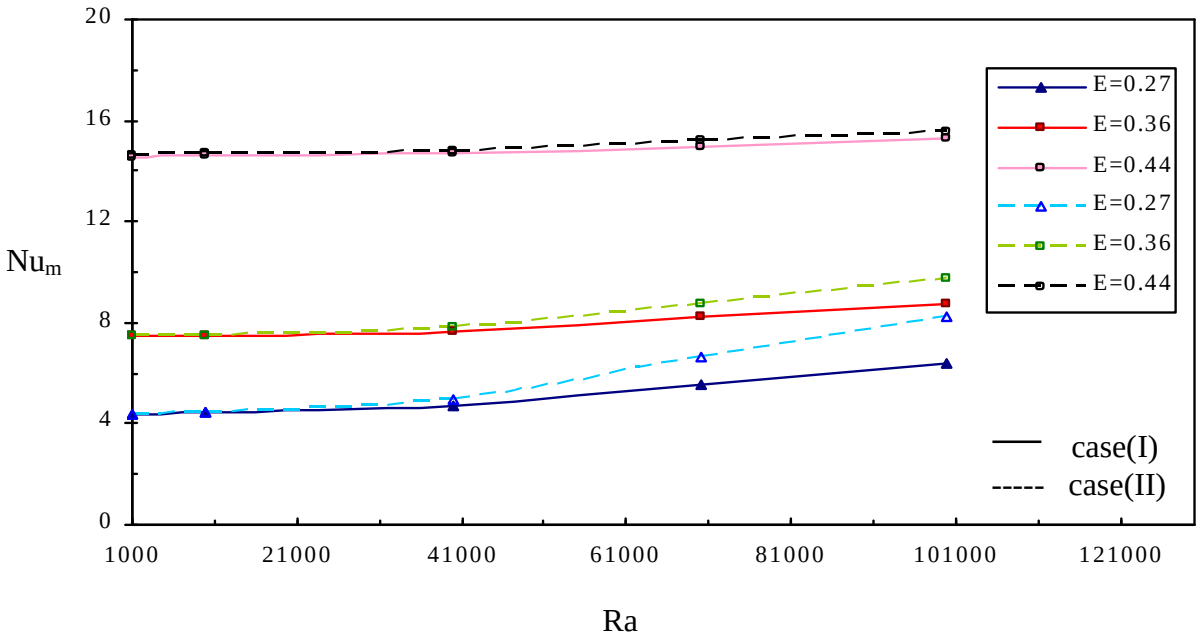

Fig.10 Variation of the mean Nusselt number with Rayleigh number along the outer wall for different values of E